



Neutrino masses and Hubble tension via a Majoron in MFV

Fernando Arias-Aragón^{1,2,a}, Enrique Fernández-Martínez^{1,2,b}, Manuel González-López^{1,2,c} , Luca Merlo^{1,2,d}

¹ Instituto de Física Teórica UAM/CSIC, Calle Nicolás Cabrera 13-15, Cantoblanco, 28049 Madrid, Spain

² Departamento de Física Teórica, Universidad Autónoma de Madrid, Cantoblanco, 28049 Madrid, Spain

Received: 25 September 2020 / Accepted: 28 December 2020 / Published online: 15 January 2021

© The Author(s) 2021

Abstract The recent tension between local and early measurements of the Hubble constant can be explained in a particle physics context. A mechanism is presented where this tension is alleviated due to the presence of a Majoron, arising from the spontaneous breaking of Lepton Number. The lightness of the active neutrinos is consistently explained. Moreover, this mechanism is shown to be embeddable in the minimal (Lepton) flavour violating context, providing a correct description of fermion masses and mixings, and protecting the flavour sector from large deviations from the Standard Model predictions. A QCD axion is also present to solve the Strong CP problem. The Lepton Number and the Peccei–Quinn symmetries naturally arise in the minimal (Lepton) flavour violating setup and their spontaneous breaking is due to the presence of two extra scalar singlets. The Majoron phenomenology is also studied in detail. Decays of the heavy neutrinos and the invisible Higgs decay provide the strongest constraints in the model parameter space.

1 Introduction

There is nowadays a considerable tension between late-time, local probes of the present rate of expansion of the Universe, that is the Hubble constant H_0 , and its value inferred through the standard cosmological model Λ CDM from early Universe observations. Local measurements, from type-Ia supernovae and strong lensing, tend to cluster at similar values of H_0 , significantly larger than those preferred by cosmic microwave background (CMB) and baryon acoustic oscillations probes. The strongest tension, estimated at the level of $4 - 6 \sigma$ [1,2] depending on the assumptions performed, is between the Planck inferred measure from the CMB spec-

trum [3] and the one obtained by the SH_0ES collaboration [4] from supernovae measurements.

Although the solution to this discrepancy might be related to systematics in the measurements (notably the calibration of the supernovae distances) or, more interestingly, point to a modification of the cosmological model, it may instead be provided by particle physics, as already discussed in the literature (see for example [5–18]). In particular, Ref. [14] suggests that a Majoron that couples to light neutrinos could reduce the tension in the determination of H_0 . It is then interesting to investigate whether this setup is compatible with possible explanations of other open problems in the Standard Model of particle physics (SM): the focus of this paper is to study the compatibility with Type-I Seesaw mechanism to explain the lightness of the active neutrinos, with specific flavour symmetries to describe the flavour puzzle and with the presence of an axion to solve the strong CP problem.

The Majoron, called ω hereafter, is the Nambu–Goldstone boson (NGB) associated to the spontaneous breaking of lepton number (LN) [19–22], which is only accidental within the SM and breaks down at the quantum level. It naturally arises in the context of the Type-I Seesaw mechanism, where the Majorana mass term, instead of being a simple bilinear of the right-handed (RH) neutrino fields N_R , is a Yukawa-like term that couples N_R to a scalar field that carries a LN charge, labelled as χ in the following. Once this scalar field develops a vacuum expectation value (VEV), then LN is spontaneously broken, a Majorana neutrino mass term is generated and the Majoron appears as a physical degree of freedom of the spectrum.

If a Dirac term that mixes N_R and the left-handed (LH) lepton doublets ℓ_L is also present in the Lagrangian, small masses for active neutrinos are generated at low energies, according to the Type-I Seesaw mechanism.

At low-energies, the Majoron ω acquires a coupling with ν_L , labelled as $\lambda_{\omega\nu\nu}$. For Majoron masses

$$m_\omega \in [0.1, 1] \text{ eV} \quad (1.1)$$

^a e-mail: fernando.arias@uam.es

^b e-mail: enrique.fernandez-martinez@uam.es

^c e-mail: manuel.gonzalezl@uam.es (corresponding author)

^d e-mail: luca.merlo@uam.es

and $\lambda_{\omega\nu\nu}$ in the range

$$\lambda_{\omega\nu\nu} \in [5 \times 10^{-14}, 10^{-12}], \quad (1.2)$$

the tension on the Hubble constant is reduced [14]. Indeed, for such small Majoron-neutrino mixings and Majoron masses, Majorons only partially thermalise after Big Bang Nucleosynthesis (BBN) or never thermalise [23], enhancing the effective number of neutrino species N_{eff} by at least 0.03 and at most 0.11, values that may be tested with CMB-S4 experiments [24]. Moreover, a non-vanishing $\lambda_{\omega\nu\nu}$ would reduce neutrino free-streaming, modifying the neutrino anisotropic stress energy tensor [25]. This has an impact in the CMB that results in modifying the posterior for the Hubble constant: as shown in Ref. [14], the inclusion of Majoron-neutrino interactions slightly shifts the central value of H_0 , but largely broadens its profile reducing the H_0 tension to 2.5σ . For larger couplings, $\lambda_{\omega\nu\nu} > 10^{-12}$, these effects are too large and excluded by the same Planck data.

Interestingly, Ref. [14] found that the best χ^2 in a Markov Chain Monte Carlo corresponds to Majoron mass and coupling as in Eqs. (1.1) and (1.2) and $\Delta N_{\text{eff}} = 0.52 \pm 0.19$. The uncertainty in the last observable is very large and $\Delta N_{\text{eff}} = 0$ is compatible within 3σ . However, values close to the central one can be achieved if a thermal population of Majorons is produced in the early Universe and is not diluted during inflation. This may occur if the reheating temperature is larger than the RH neutrino masses [14]. Alternatively, other relativistic species, such as axions [26–29], may contribute to ΔN_{eff} and their presence may justify such a large value.

The existence of both Majorana and Dirac terms, the achievement of the correct scale for the active neutrino masses and at the same time the alleviation of the Hubble tension via the Majoron strongly depend on the LN charge assignments of ℓ_L , N_R and χ . In particular, fixing the LN of ℓ_L to unity, then the LN of the RH neutrinos needs to have opposite sign with respect to the LN of the scalar field χ . This model presents interesting phenomenological features. On one hand, the heavy neutrinos are expected to be relatively light, with masses at the MeV or GeV scales, opening up the possibility to be studied at colliders. Moreover, the presence of the Majoron may also have other consequences distinct from the Hubble tension. In particular, its couplings to photons and electrons are constrained by CAST and Red Giant observations, respectively, while, due to its coupling to the Higgs, the Majoron may contribute to the invisible Higgs decay, strongly constrained by colliders.

Section 2 illustrates the mechanism to produce a Majoron that alleviates the H_0 tension together with a correct scale for the active neutrino masses. In Sect. 3, this mechanism is introduced in a setup that correctly describes the flavour puzzle of the SM and at the same time produces a QCD axion that solves the Strong CP problem. Section 4 gathers

Table 1 LN assignments. Fields that are not listed here do not transform under LN

Field	$U(1)_L$ Charge
ℓ_L, e_R	1
N_R	$-L_N$
χ	L_χ

the phenomenological signatures of this model and Sect. 5 contains the final remarks.

2 The Majoron mechanism

To produce a Majoron and explain the lightness of the active neutrinos, one can consider a Type-I Seesaw mechanism where the Majorana mass is dynamically generated by the spontaneous breaking of LN. The SM spectrum is extended by three RH neutrinos¹ and a singlet scalar field χ that only transforms under LN. The LN charge assignments can be read in Table 1, where ℓ_L , N_R and χ have already been defined, and e_R refers to the RH charged leptons. Notice that L_χ and L_N are integer numbers and are not completely free, but must obey a series of constraints that will be made explicit in the following.

The most general effective Lagrangian in the neutrino sector invariant under LN is the following²:

$$-\mathcal{L}_\nu = \left(\frac{\chi}{\Lambda_\chi}\right)^{\frac{1+L_N}{L_\chi}} \bar{\ell}_L \tilde{H} \mathcal{Y}_\nu N_R + \frac{1}{2} \left(\frac{\chi}{\Lambda_\chi}\right)^{\frac{2L_N-L_\chi}{L_\chi}} \chi \bar{N}_R^c \mathcal{Y}_N N_R + \text{h.c.}, \quad (2.2)$$

where H is the SM Higgs doublet, $\tilde{H} = i\sigma_2 H^*$, Λ_χ is the cut-off scale up to which the effective operator approach holds, and \mathcal{Y}_ν is a dimensionless and complex matrix, while \mathcal{Y}_N is dimensionless, complex and symmetric. A first condition on $L_{N,\chi}$ arises from requiring that all the terms are local:

$$\frac{1+L_N}{L_\chi}, \frac{2L_N-L_\chi}{L_\chi} \in \mathbb{N}. \quad (2.3)$$

¹ The case with only two RH neutrinos is also viable, and correspondingly the lightest active neutrino would be massless.

² Other terms can be added to this Lagrangian inserting χ^\dagger instead of χ . However, once the terms in Eq. (2.2) are local, then their siblings with χ^\dagger would not be local and therefore cannot be added to the Lagrangian. The only exception is the term

$$\frac{1}{2} \left(\frac{\chi}{\Lambda_\chi}\right)^{\frac{2L_N+L_\chi}{L_\chi}} \chi^\dagger \bar{N}_R^c \mathcal{Y}_N N_R, \quad (2.1)$$

that however only provides a suppressed correction with respect to the Majorana term written in Eq. (2.2) and for this reason it can be neglected.

In the LN broken phase, the field χ can be parametrised as

$$\chi = \frac{\sigma + v_\chi}{\sqrt{2}} e^{i \frac{\omega}{v_\chi}}, \quad (2.4)$$

where the angular part ω is the NGB identified as a Majoron, σ is the radial component and v_χ is its VEV. Notice that the scale appearing in the denominator of the exponent is also v_χ in order to obtain canonically normalised kinetic terms for the Majoron. A useful notation that will be employed in the following is the ratio of the χ VEV and the cut-off scale:

$$\varepsilon_\chi = \frac{v_\chi}{\sqrt{2}\Lambda_\chi}. \quad (2.5)$$

This parameter ε_χ is expected to be smaller than 1 in order to guarantee a good expansion in terms of $1/\Lambda_\chi$. Consequently, the χ VEV, which represents the overall scale of the LN breaking, is expected to be smaller than the scale Λ_χ , where New Physics should be present and is responsible for generating the expression in Eq. (2.2).

Once the electroweak symmetry is also spontaneously broken, i.e. after that the SM Higgs develops its VEV that in the unitary gauge reads

$$H = \frac{h + v}{\sqrt{2}}, \quad (2.6)$$

where h is the physical Higgs and $v \simeq 246$ GeV, masses for the active neutrinos are generated according to the Type-I Seesaw mechanism:

$$\begin{aligned} \mathcal{L}_v^{\text{low-energy}} &= \frac{1}{2} \bar{\nu}_L m_\nu \nu_L^c + \text{h.c.} \quad \text{with} \\ m_\nu &= \frac{\varepsilon_\chi^{\frac{2+L_\chi}{L_\chi}} v^2}{\sqrt{2} v_\chi} \mathcal{Y}_\nu \mathcal{Y}_N^{-1} \mathcal{Y}_\nu^T. \end{aligned} \quad (2.7)$$

In the basis where the charged lepton mass matrix is already diagonal, the neutrino mass matrix can be diagonalised by the PMNS matrix U :

$$\hat{m}_\nu \equiv \text{diag}(m_1, m_2, m_3) = U^\dagger m_\nu U^*. \quad (2.8)$$

The overall scale for the active neutrino masses can be written in terms of the parameter ε_χ , the ratio of the VEVs and the product $\mathcal{Y}_\nu \mathcal{Y}_N^{-1} \mathcal{Y}_\nu^T$:

$$\frac{\varepsilon_\chi^{\frac{2+L_\chi}{L_\chi}} v^2}{\sqrt{2} v_\chi} \mathcal{Y}_\nu \mathcal{Y}_N^{-1} \mathcal{Y}_\nu^T \simeq \sqrt{|\Delta m_{\text{atm}}^2|}, \quad (2.9)$$

where $\Delta m_{\text{atm}}^2 = 2.514_{-0.027}^{+0.028} \times 10^{-3} \text{ eV}^2$ for the Normal Ordering (NO) of the neutrino mass spectrum and

$\Delta m_{\text{atm}}^2 = -2.497 \pm 0.028 \times 10^{-3} \text{ eV}^2$ for the Inverted Ordering (IO) [30].

The heavy neutrinos, that mostly coincide with the RH neutrinos, have a mass matrix that in first approximation can be directly read from the Lagrangian in Eq. (2.2),

$$M_N \simeq \varepsilon_\chi^{\frac{2L_N-L_\chi}{L_\chi}} \frac{v_\chi}{\sqrt{2}} \mathcal{Y}_N. \quad (2.10)$$

The overall scale for the heavy neutrinos must be larger than the overall scale of the active neutrinos, in order for the Seesaw approximation to hold:

$$\varepsilon_\chi^{\frac{2L_N-L_\chi}{L_\chi}} \frac{v_\chi}{\sqrt{2}} \mathcal{Y}_N \gg \sqrt{|\Delta m_{\text{atm}}^2|}. \quad (2.11)$$

On the other hand, the electroweak and LN breakings give rise to the Majoron Lagrangian that can be written as follows:

$$\begin{aligned} \mathcal{L}_\omega &= \frac{1}{2} \partial_\mu \omega \partial^\mu \omega + \frac{1}{2} m_\omega^2 \omega^2 - i \frac{1+L_N}{L_\chi} \varepsilon_\chi^{\frac{1+L_N}{L_\chi}} \frac{v}{\sqrt{2} v_\chi} \bar{\nu}_L \mathcal{Y}_\nu N_R \omega + \\ &\quad - i \frac{L_N}{L_\chi} \varepsilon_\chi^{\frac{2L_N-L_\chi}{L_\chi}} \frac{\bar{N}_R^c \mathcal{Y}_N N_R \omega}{\sqrt{2}} + \text{h.c.}, \end{aligned} \quad (2.12)$$

where the m_ω^2 term parametrises the Majoron mass introduced here as an explicit breaking of its corresponding shift symmetry. At low energy, a direct coupling of the Majoron to the active neutrinos emerges after performing the same transformations that give rise to the mass matrix in Eq. (2.7):

$$\mathcal{L}_\omega^{\text{low-energy}} \supset i \frac{\lambda_{\omega\nu\nu}}{2} \omega \bar{\nu}_L \nu_L^c + \text{h.c.} \quad \text{with} \quad \lambda_{\omega\nu\nu} = 2 \frac{m_\nu}{L_\chi v_\chi}. \quad (2.13)$$

³From the results in Ref. [14], shown in Eq. (1.2), it is then possible to infer a bound on the product $L_\chi v_\chi$, once taking $\sqrt{|\Delta m_{\text{atm}}^2|}$ as the overall scale for the neutrino masses:

$$|L_\chi| v_\chi \simeq \frac{2\sqrt{|\Delta m_{\text{atm}}^2|}}{\lambda_{\omega\nu\nu}} \in [0.1, 2] \text{ TeV}. \quad (2.14)$$

Adopting this relation and substituting it within the expressions in Eqs. (2.9) and (2.11), new conditions can be found:

$$\begin{aligned} |L_\chi| \varepsilon_\chi^{\frac{2+L_\chi}{L_\chi}} \mathcal{Y}_\nu \mathcal{Y}_N^{-1} \mathcal{Y}_\nu^T \\ \simeq \frac{2\sqrt{2}}{\lambda_{\omega\nu\nu}} \frac{|\Delta m_{\text{atm}}^2|}{v^2} \in [1.2 \times 10^{-13}, 2.4 \times 10^{-12}], \end{aligned} \quad (2.15)$$

³ This expression coincides with the one in Ref. [14] once identifying ω with ϕ and $\lambda_{\omega\nu\nu}$ with λ .

$$\frac{\epsilon_\chi}{|L_\chi|} \mathcal{Y}_N \gg \frac{\lambda_{\omega\nu\nu}}{\sqrt{2}} \simeq 3.5 \times 10^{-14}. \quad (2.16)$$

The following choice of charge assignments leads to a completely renormalisable Lagrangian and thus deserves special mention:

$$\text{CASE R: } L_N = -1 \quad \text{and} \quad L_\chi = -2, \quad (2.17)$$

such that the powers of the ratio χ/Λ_χ in Eq. (2.2) are not present in either the Dirac and the Majorana terms. The relation in Eq. (2.14) and the two conditions in Eqs. (2.15) and (2.16) further simplify:

$$\text{Eq. (2.14)} \longrightarrow v_\chi \simeq \frac{\sqrt{|\Delta m_{\text{atm}}^2|}}{\lambda_{\omega\nu\nu}} \in [0.05, 1] \text{ TeV}. \quad (2.18)$$

$$\begin{aligned} \text{Eq. (2.15)} \longrightarrow \mathcal{Y}_\nu \mathcal{Y}_N^{-1} \mathcal{Y}_\nu^T &\simeq \frac{\sqrt{2}}{\lambda_{\omega\nu\nu}} \frac{|\Delta m_{\text{atm}}^2|}{v^2} \\ &\in [1.2 \times 10^{-13}, 2.4 \times 10^{-12}], \end{aligned} \quad (2.19)$$

$$\text{Eq. (2.16)} \longrightarrow \mathcal{Y}_N \gg \frac{2\lambda_{\omega\nu\nu}}{\sqrt{2}} \simeq 7 \times 10^{-13}. \quad (2.20)$$

The first expression fixes a range of values for v_χ . While the third expression represents a lower bound on the overall scale of \mathcal{Y}_N , the second one implies that the product $\mathcal{Y}_\nu \mathcal{Y}_N^{-1} \mathcal{Y}_\nu^T$ should be tuned to a very small value in order to reproduce the lightness of the active neutrinos.

For values of $L_{N,\chi}$ different from the previous ones, the Lagrangian is necessarily non-renormalisable. An interesting question is whether the extremely small values of the product $\mathcal{Y}_\nu \mathcal{Y}_N^{-1} \mathcal{Y}_\nu^T$ can be avoided exploiting the suppression in ϵ_χ from the new physics scale Λ_χ , similarly to the Froggatt-Nielsen approach to the flavour puzzle [31]. Considering first the case in which $L_{N,\chi} > 0$, then the only available possibilities are

$$\begin{aligned} \text{CASE NR1: } L_N = 1 \quad \text{and} \quad L_\chi = 1 \\ \text{CASE NR2: } L_N = 1 \quad \text{and} \quad L_\chi = 2. \end{aligned} \quad (2.21)$$

The corresponding values for v_χ, ϵ_χ , the overall scale for the heavy neutrinos $\langle M_N \rangle$ and the cut-off scale Λ_χ are reported in Table 2.

From Eq. (2.15), it can be seen that ϵ_χ gets smaller for larger values of L_χ (unless tuning the product $\mathcal{Y}_\nu \mathcal{Y}_N^{-1} \mathcal{Y}_\nu^T$ as in CASE R discussed above, a possibility to be avoided in the present discussion): although this is not a problem by itself, it hardens the constraint in Eq. (2.16). It follows that for larger values of L_N and L_χ satisfying to the locality conditions in Eq. (2.3), then the overall scale of the heavy neutrino masses would be as small as the one of active neutrinos and therefore the expansion in the Type-I Seesaw mechanism would break down.

In the case when $L_N > 0$ and $L_\chi < 0$, it is possible to obtain the same results listed above substituting χ by χ^\dagger in the Lagrangian in Eq. (2.2): in this case, the signs in the denominators of the exponents would be flipped, compensating the negative sign of L_χ . The opposite case, $L_N < 0$ and $L_\chi > 0$, is not allowed by the locality conditions.

For $L_{N,\chi} < 0$, besides the possibility of CASE R, only another choice is allowed by the locality conditions: ($L_N = -1, L_\chi = -1$). However, this case would require $\epsilon_\chi \gg 1$, leading to an even more extreme fine-tuning than in CASE R without the appeal of renormalizability.

The condition in Eq. (2.14), corresponding to Eq. (1.2), is only one of the ingredients necessary to lower the H_0 tension. A second relevant requirement is Eq. (1.1), regarding the Majoron mass. For the sake of simplicity, it has been introduced directly in the Majoron Lagrangian in Eq. (2.12) as an effective term. Its origin has been widely discussed in the literature and constitutes in itself an interesting research topic. Any violation of the global LN symmetry would induce a mass for the Majoron. An obvious example are gravitational effects, which are expected to break all accidental global symmetries. Estimations of their size from non-perturbative arguments via wormhole effects [32] fall too short of their required value. Conversely, their size from Planck-suppressed effective operators [33] would point to too large a mass, although several possibilities have been discussed that would prevent the lower dimension operators from being generated [34–41]. These options were originally introduced as a solution to the axion quality problem. A simpler possibility, given the singlet nature of the N_R , is an explicit breaking of LN via a Majorana mass term at the Lagrangian level. The Majoron would thus develop a mass slightly below this breaking scale from its coupling to the N_R through self-energy diagrams. In this work we will remain agnostic to the origin of the Majoron mass, and a value consistent with Eq. (1.1) will be assumed.

Besides the Majoron, also the radial component of χ is present in the spectrum and does play a role modifying the Higgs scalar potential. Indeed, the most general scalar potential containing H and χ can be written as

$$V(H, \chi) = -\mu^2 H^\dagger H + \lambda (H^\dagger H)^2 - \mu_\chi^2 \chi^* \chi + \lambda_\chi (\chi^* \chi)^2 + g H^\dagger H \chi^* \chi \quad (2.22)$$

The minimisation of such potential leads to VEVs for the two fields that read

$$v^2 = \frac{4\lambda_\chi \mu^2 - 2g\mu_\chi^2}{4\lambda\lambda_\chi - g^2}, \quad v_\chi^2 = \frac{4\lambda\mu_\chi^2 - 2g\mu^2}{4\lambda\lambda_\chi - g^2}. \quad (2.23)$$

The parameters of this scalar potential need to be such that v takes the electroweak value and v_χ acquires the values in Table 2.

Table 2 Parameter ranges in the two phenomenologically interesting scenarios

	L_N	L_χ	v_χ	ε_χ	$\langle M_N \rangle$	Λ_χ
CASE NR1	1	1	[0.1, 2] TeV	$[0.49, 1.4] \times 10^{-4}$	[3.5, 200] MeV	$[1.4 - 11] \times 10^3$ TeV
CASE NR2	1	2	[0.05, 1] TeV	$[2.4, 11] \times 10^{-7}$	[35.4, 707] GeV	$[1.4 - 6.5] \times 10^5$ TeV

Due to the mixed quartic term, the two physical scalar fields h and σ mix in the broken phase and the mass matrix describing this mixing is given by

$$\mathcal{M}^2 = \begin{pmatrix} 2\lambda v^2 & g v v_\chi \\ g v v_\chi & 2\lambda_\chi v_\chi^2 \end{pmatrix}. \quad (2.24)$$

The two eigenvalues that arise after diagonalising this mass matrix are the following

$$M_{h,\sigma}^2 = \lambda v^2 + \lambda_\chi v_\chi^2 \pm \left(\lambda v^2 - \lambda_\chi v_\chi^2 \right) \sqrt{1 + \tan^2 2\vartheta}, \quad (2.25)$$

where

$$\tan 2\vartheta = \frac{g v v_\chi}{\lambda_\chi v_\chi^2 - \lambda v^2}. \quad (2.26)$$

The lightest mass in Eq. (2.25) corresponds to the eigenstate mainly aligned with the SM Higgs, while the heaviest state is mainly composed of the radial component of χ . Its mass can be as small as a few hundred GeV or much larger than the TeV. From the relation between the mixed quartic coupling g and the physical parameters,

$$g = \frac{M_\sigma^2 - M_h^2}{2 v v_\chi} \sin 2\vartheta, \quad (2.27)$$

it is possible to straightforwardly study the dependence of M_σ with the other model parameters. Notice that the mixing parameter ϑ is constrained by LHC data to be [42]

$$\sin^2 \vartheta \lesssim 0.11, \quad (2.28)$$

from a $\sqrt{s} = 13$ TeV analysis of Higgs signal strengths with 80 fb^{-1} of integrated luminosity.

As shown in Fig. 1, M_σ can reach very large values, without requiring any fine-tuning on g . On the contrary, very small M_σ can only be achieved for g close to zero. It is then natural to focus on the case in which σ is massive enough to be safely integrated out. This will be the case in the rest of the paper.

The mechanism illustrated in this section allows to soften the H_0 tension explaining at the same time the lightness of the active neutrinos. In the next section, this mechanism will be embedded into a specific flavour model that allows to account for the flavour puzzle, without violating any bounds

from flavour observables, and also contains a QCD axion that solves the strong CP problem.

3 The Majoron and Axion from a MFV setup

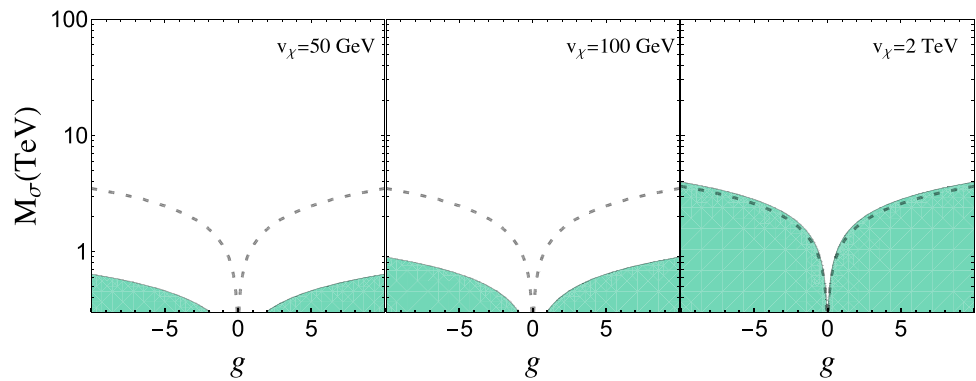
Flavour models aim at describing the heterogeneity of the fermion masses and mixings through some underlying argument, such as a symmetry principle. The simplest proposal is known as the Froggatt–Nielsen model [31] and consists in introducing a global Abelian symmetry to describe the flavour structure in the quark sector. Almost 25 years later, after the more precise measurements of neutrino oscillations and the introduction of the so-called tri-bimaximal mixing texture [43,44], whose main feature is a vanishing reactor mixing angle in the PMNS matrix, discrete symmetries were considered as an attractive approach to reproduce the observed pattern of all fermion masses and mixings [45–52]. However, after the discovery, in 2011, of a relatively large reactor mixing angle [53–57], models based on discrete symmetries underwent a deep rethinking and other options also became popular. A few examples are Froggatt–Nielsen inspired models based on a simple $U(1)$ [58–60] and models based on continuous non-Abelian symmetries. The latter include Minimal Flavour Violation (MFV) [61] and its leptonic versions [62–64], which are based on a $U(3)$ symmetry, smaller symmetries like $U(2)$ [65,66], or an intermediate approach [67].

The focus here will be the MFV setup, that will be shown to naturally suggest the presence of the Majoron and of a QCD axion. The key concept behind MFV is to require that any flavour and CP violation in physics Beyond the SM has the same origin as the one in the SM [68]. This idea has been formulated in terms of the symmetries of the kinetic terms in Ref. [61]. These symmetries are then broken by a series of fields that are also employed to describe fermion masses and mixings, as well as the suppressions associated to any non-renormalisable flavour violating operator. Considering the SM spectrum augmented by three RH neutrinos, the flavour symmetry of the corresponding kinetic terms is a product of a $U(3)$ term for each fermion species,

$$\mathcal{G}_F = U(3)^6. \quad (3.1)$$

The non-Abelian terms are responsible for the intergenerational fermion mass hierarchies and of the mixing matri-

Fig. 1 M_σ vs. g parameter space, fixing $v = 246$ GeV, $M_h = 125$ GeV and taking three values for LN breaking scale, $v_\chi = \{50 \text{ GeV}, 100 \text{ GeV}, 2 \text{ TeV}\}$. The white area is the one allowed by the bound in Eq. (2.28), while the green region is the excluded one. The dashed line correspond to the bound in Eq. (4.13), being the area above such line allowed



ces, while the Abelian terms are associated to the hierarchies among the masses of the different third family fermions. The latter can be written as follows

$$\mathcal{G}_F^A = U(1)_{q_L} \times U(1)_{u_R} \times U(1)_{d_R} \times U(1)_{\ell_L} \times U(1)_{e_R} \times U(1)_{N_R}, \quad (3.2)$$

where q_L refers to the LH quark doublets, u_R to the RH up-type quarks and d_R to the RH down-type quarks, while ℓ_L , e_R and N_R to the leptons as already introduced in the previous section. It is possible to rearrange this product, provided that the new combinations are still linearly independent, identifying among them baryon number, LN, weak hypercharge and the Peccei–Quinn (PQ) [69] symmetry:

$$\mathcal{G}_F^A = U(1)_B \times U(1)_L \times U(1)_Y \times U(1)_{PQ} \times U(1)_{e_R} \times U(1)_{N_R}. \quad (3.3)$$

In the model described in this section, fermion charges under baryon number and hypercharge are assigned as in the SM, while the LN charges are given in Table 1. Moreover, PQ charges are chosen so as to explain the suppression of the bottom and τ masses with respect to the top mass: only d_R and e_R transform under PQ, with a charge equal to 3. In an analogous way to LN, the PQ symmetry is formally exact at the Lagrangian level after introducing a second scalar field Φ that transforms non-trivially only under PQ with a charge -1 :

$$\Phi = \frac{\rho + v_\Phi}{\sqrt{2}} e^{i \frac{a}{v_\Phi}}, \quad (3.4)$$

where ρ is the radial component, a is the angular one and v_Φ is its VEV. Once this scalar field develops a VEV and electroweak symmetry gets broken, masses for bottom and τ are generated, suppressed with respect to the top one. As a byproduct of this mechanism, the axion a is originated [70]. Finally, the last two symmetries in Eq. (3.3) do not play any role in this model and are explicitly broken.

The Lagrangian invariant under the aforementioned symmetries is the following:

$$\begin{aligned} -\mathcal{L}_Y = & \bar{q}_L \tilde{H} \mathcal{Y}_u u_R + \left(\frac{\Phi}{\Lambda_\Phi} \right)^3 \bar{q}_L H \mathcal{Y}_d d_R + \left(\frac{\Phi}{\Lambda_\Phi} \right)^3 \bar{\ell}_L H \mathcal{Y}_e e_R \\ & + \left(\frac{\chi}{\Lambda_\chi} \right)^{\frac{1+x_N}{x_\chi}} \bar{\ell}_L \tilde{H} \mathcal{Y}_\nu N_R \\ & + \frac{1}{2} \left(\frac{\chi}{\Lambda_\chi} \right)^{\frac{2x_N-x_\chi}{x_\chi}} \chi \bar{N}_R^c \mathcal{Y}_N N_R + \text{h.c.}, \end{aligned} \quad (3.5)$$

where Λ_Φ stands for the cut-off scale associated to the scalar field Φ .

According to the MFV approach, $\mathcal{Y}_{u,d,e,v,N}$ are not simple matrices, but are promoted to be spurion fields that do transform under the non-Abelian part of the flavour symmetry group \mathcal{G}_F . These fields can be thought of as dimensionless scalar fields that do not have kinetic terms, but acquire background values that play the role of VEVs. In the MFV approach, to reproduce correctly quark masses and mixings and charged lepton masses, the background values of $\mathcal{Y}_{u,d,e}$ should read

$$\begin{aligned} \langle \mathcal{Y}_u \rangle &= c_t V^\dagger \text{diag} \left(\frac{m_u}{m_t}, \frac{m_c}{m_t}, 1 \right), \\ \langle \mathcal{Y}_d \rangle &= c_b \text{diag} \left(\frac{m_d}{m_b}, \frac{m_s}{m_b}, 1 \right), \\ \langle \mathcal{Y}_e \rangle &= c_\tau \text{diag} \left(\frac{m_e}{m_\tau}, \frac{m_\mu}{m_\tau}, 1 \right), \end{aligned} \quad (3.6)$$

where V is the CKM mixing matrix and c_i are order 1 parameters. The possible origin of these values is under study [71–74].

While these matrices present hierarchies among their entries, the ratios m_b/m_t and m_τ/m_t are still not described within this approach, but can be explained by the spontaneous breaking of the PQ symmetry. Indeed, the overall scale of down-type quarks and charged leptons is multiplied by the cubic power of the ratio among the Φ VEV and the cut-off

Λ_Φ . Assuming that this ratio is given by

$$\frac{v_\Phi}{\sqrt{2}\Lambda_\Phi} \simeq 0.23, \quad (3.7)$$

the m_b/m_t and m_τ/m_t ratios are also correctly described.

Any non-renormalisable operator that describes flavour-violating processes should be invariant under the flavour symmetry. This is accomplished by inserting proper powers of the spurions: once they acquire their background values, the non-renormalisable operator under consideration gets suppressed. The main consequence is that the scale that can be studied considering flavour observables is at the level of 1–10 TeV [61, 75–85], instead of 100 TeV in a generic case [86], opening up the possibility of discovering New Physics (NP) at colliders.

For the neutrino sector, the discussion is slightly more complicated. Indeed, there are two spurions in the neutrino sector, \mathcal{Y}_ν and \mathcal{Y}_N , and both enter in the definition of the active neutrino masses, see Eq. (2.7). It follows that it is not possible to identify univocally either \mathcal{Y}_ν or \mathcal{Y}_N in terms of neutrino masses and the PMNS matrix entries. Thus, the suppression in the non-renormalisable flavour violating operators cannot be directly linked to neutrino masses and mixings, losing the predictivity that characterizes the MFV approach in the quark sector. The solutions that have been proposed are to assume $\mathcal{Y}_N \propto \mathbb{1}$ [62, 63] or to consider \mathcal{Y}_ν as a unitary matrix [64].

I): $\mathcal{G}_L^{NA} \rightarrow SU(3)_{\ell_L} \times SU(3)_{e_R} \times SO(3)_{N_R} \times CP$ [62, 63].

Under the assumption that the three RH neutrinos are degenerate in mass, i.e. $\mathcal{Y}_N \propto \mathbb{1}$, then the non-Abelian symmetry associated to the RH neutrinos, $SU(3)_{N_R}$, is broken down to $SO(3)_{N_R}$. The additional assumption of no CP violation in the lepton sector is meant to force Y_ν to be real⁴. With these simplifications, the expression for the active neutrino mass in Eq. (2.7) simplifies to

$$m_\nu = \frac{\varepsilon_\chi^{\frac{2+L_\chi}{L_\chi}} v^2}{\sqrt{2}v_\chi} \mathcal{Y}_\nu \mathcal{Y}_\nu^T, \quad (3.8)$$

and all flavour changing effects involving leptons can be written in terms of $\mathcal{Y}_\nu \mathcal{Y}_\nu^T$ and Y_e . These are the only relevant combinations entering any $d = 6$ operator involving lepton fields and describing flavour violating effects. It follows that any flavour changing process can be predicted in terms of lepton masses and mixings.

⁴ Strictly speaking, the condition of CP conservation in the leptonic sector forces the Dirac CP phase to be equal to $\delta_{CP}^\ell = \{0, \pi\}$ and the Majorana CP phases to be $\alpha_{21,31} = \{0, \pi, 2\pi\}$. However, Y_ν is real only if $\alpha_{21,31} = \{0, 2\pi\}$, and therefore $\alpha_{21,31} = \pi$ needs to be disregarded in order to guarantee predictivity. The CP conservation condition assumed in Refs. [62, 63] is then stronger than the strict definition.

Diagonalising m_ν corresponds to diagonalising the product $\langle \mathcal{Y}_\nu \rangle \langle \mathcal{Y}_\nu \rangle^T$ and, given the fact that the lepton mixing angles are relatively large, then no hierarchies should be expected among the entries of $\langle \mathcal{Y}_\nu \rangle \langle \mathcal{Y}_\nu \rangle^T$, contrary to what happens in the quark case. Note that some setups, such as the so-called sequential dominance scenarios, obtain large mixing angles even if there exists a strong hierarchy among the Yukawa couplings [87]. However, this possibility is disfavoured by the general philosophy of MLFV. In the same spirit, the overall scale of this product is of $\mathcal{O}(1)$, as any explanation of the neutrino masses should reside in the model itself, and not be due to any fine-tuning.

II): $\mathcal{G}_L^{NA} \rightarrow SU(3)_{\ell_L+N_R} \times SU(3)_{e_R}$ [64].

Assuming that the three RH neutrinos transform as a triplet under the same symmetry group of the lepton doublets,

$$\ell_L, N_R \sim (\mathbf{3}, 1)_{\mathcal{G}_L^{NA}} \quad e_R \sim (1, \mathbf{3})_{\mathcal{G}_L^{NA}}, \quad (3.9)$$

then Schur's Lemma guarantees that \mathcal{Y}_ν transforms as a singlet of the symmetry group. Then, Y_ν is a unitary matrix [88, 89], which can always be rotated to the identity matrix by a suitable unitary transformation acting only on the RH neutrinos. The only meaningful quantities in this context are \mathcal{Y}_e and \mathcal{Y}_N , so neutrino masses and lepton mixings are encoded uniquely into Y_N ,

$$m_\nu = \frac{\varepsilon_\chi^{\frac{2+L_\chi}{L_\chi}} v^2}{\sqrt{2}v_\chi} \mathcal{Y}_N^{-1}. \quad (3.10)$$

Moreover, all flavour changing effects involving leptons can be written only in terms of Y_e and Y_N , and therefore any flavour changing process can be predicted in terms of lepton masses and mixings.

As for the previous case, the diagonalisation of the active neutrino mass coincides with the diagonalisation of $\langle \mathcal{Y}_N \rangle^{-1}$, that therefore does not present any strong hierarchy among its entries. Moreover, its overall scale should be $\mathcal{O}(1)$ according to the MLFV construction approach.

In both cases, the constraints on NP considering the present available data on flavour changing processes in the lepton sector are as low as a few TeV [62–64, 90–93].

Once the PQ symmetry is spontaneously broken, the axion arises as its NGB and its Lagrangian can be written as

$$\begin{aligned} \mathcal{L}_a = & \frac{1}{2} \partial_\mu a \partial^\mu a - e^{\frac{3ia}{v_\Phi}} \bar{q}_L H \mathcal{Y}_d d_R - e^{\frac{3ia}{v_\Phi}} \bar{\ell}_L H \mathcal{Y}_e e_R \\ & + \frac{\alpha_s}{8\pi} \theta_{\text{QCD}} G^{a\mu\nu} \tilde{G}_{\mu\nu}^a, \end{aligned} \quad (3.11)$$

with $\tilde{G}_{\mu\nu}^a \equiv \frac{1}{2}\epsilon_{\mu\nu\rho\sigma}G^{a\rho\sigma}$ and $\epsilon_{\mu\nu\rho\sigma}$ the totally antisymmetric tensor such that $\epsilon_{1230} = 1$. The last term is the well-known QCD θ -term, allowed by the QCD Lagrangian, which constitutes a source of CP violation. The θ_{QCD} parameter contributes to the neutron electric dipole moment [94,95] and can thus be experimentally constrained [96]

$$\theta_{\text{QCD}} \lesssim 10^{-10}. \quad (3.12)$$

The presence of the axion naturally explains why θ_{QCD} is so small, providing a solution to the Strong CP problem: couplings of the axion to the gauge fields, and in particular to gluons, are generated at the quantum level and the θ_{QCD} parameter can be reabsorbed by an axion field redefinition [69,97,98]. The effective axion potential (see for example Ref. [99]) predicts a vanishing VEV for the axion, that finally solves the Strong CP problem. Moreover, the same potential provides the axion with a mass,

$$m_a \sim 6 \mu\text{eV} \left(\frac{10^{12} \text{ GeV}}{f_a} \right), \quad (3.13)$$

being f_a the axion scale, that is connected to the Φ VEV in this model by the relation $f_a = v_\Phi/9$. For QCD axions, the most stringent constraint on f_a comes from the axion couplings to photons [100–102] and to electrons [103–105], which push its value to be larger than $f_a \gtrsim 1.2 \times 10^7 \text{ GeV}$ and $f_a \gtrsim 8 \times 10^8 \text{ GeV}$, respectively.

Summarising, the Majoron together with axion constitute the natural Abelian completion of MFV scenarios. The Majoron does not affect (at tree level) the physics associated to the axion and the quark and charged lepton flavour physics. Thus, this model, besides describing fermion masses and mixings and solving the Strong CP problem, is able to alleviate the Hubble tension with the only inclusion of three RH neutrinos and two extra singlet scalars. In particular, as no fine-tuning is allowed within this approach on $\langle \mathcal{Y}_\nu \rangle$ or $\langle \mathcal{Y}_N \rangle$, then only CASE NR1 and CASE NR2 are viable in the MFV framework. In the following section, the analysis of this model will be completed with the study of its phenomenological signatures.

4 Phenomenological signatures

The only tree-level coupling of the Majoron is to neutrinos. However, at quantum level, couplings to gauge bosons, other SM fermions and the Higgs are originated.

Coupling to photons

The searches for very light pseudoscalars, usually addressed to axions, can also apply to Majorons. In the range of masses

in Eq. (1.1), the strongest constraints on the effective coupling to photons are set by CAST [102], which establishes the upper bound

$$\lambda_{\omega\gamma\gamma} \lesssim 10^{-10} \text{ GeV}^{-1}, \quad (4.1)$$

where $\lambda_{\omega\gamma\gamma}$ is defined as

$$\mathcal{L}_\omega^{\text{low-energy}} \supset \frac{1}{4} \lambda_{\omega\gamma\gamma} \omega F^{\mu\nu} \tilde{F}_{\mu\nu} \quad (4.2)$$

with $\tilde{F}_{\mu\nu} \equiv \frac{1}{2}\epsilon_{\mu\nu\rho\sigma}F^{\rho\sigma}$.

As the Majoron does not couple at tree-level to charged particles, then the process $\omega \rightarrow \gamma\gamma$ occurs only at two loops. Ref. [106] provides an estimate for its decay width: under the assumption $m_\omega \ll m_e$,

$$\Gamma_{\omega \rightarrow \gamma\gamma} = \frac{\alpha^2}{1536^2 \pi^7} \frac{m_\omega^7}{v^2 m_e^4} \left(\text{Tr} \left[\frac{m_D m_D^\dagger}{v v_\chi} \right] \right)^2 \quad (4.3)$$

where $\alpha \equiv e^2/4\pi$ and with m_D the Dirac neutrino mass matrix.

Computing the same process by means of the effective couplings in Eq. (4.2),

$$\Gamma_{\omega \rightarrow \gamma\gamma} = \frac{\lambda_{\omega\gamma\gamma}^2 m_\omega^3}{32\pi} \quad (4.4)$$

it is then possible to match the two expressions for the $\omega \rightarrow \gamma\gamma$ decay width providing the expression for the $\lambda_{\omega\gamma\gamma}$ coupling:

$$\lambda_{\omega\gamma\gamma} = \frac{\alpha m_\omega^2}{384 \sqrt{2} \pi^3 m_e^2 v_\chi} \epsilon_\chi^{\frac{2+2L_N}{L_\chi}} \text{Tr} \left[\mathcal{Y}_\nu \mathcal{Y}_\nu^\dagger \right]. \quad (4.5)$$

Table 3 shows the numerical estimations for the predicted values of the Majoron coupling to photons, assuming that the trace gives an $\mathcal{O}(1)$ number, as already discussed: the experimental bound is still far from the theoretical prediction.

Coupling to electrons

Astrophysical measurements can also constrain Majoron couplings. Ref. [103] provides an upper bound on the Majoron effective coupling to electrons

$$\mathcal{L}_\omega^{\text{low-energy}} \supset i \lambda_{\omega ee} \omega \bar{e} e, \quad (4.6)$$

based on observations on Red Giants:

$$\lambda_{\omega ee} < 4.3 \times 10^{-13}. \quad (4.7)$$

Table 3 Predictions for the Majoron effective couplings to electrons, photons and neutrinos, for the window of the parameter space where Hubble tension is alleviated. In the last line, the corresponding experimental upper bounds

	$\lambda_{\omega\gamma\gamma}$	$\lambda_{\omega ee}$	$\lambda_{\omega\nu\nu}$
CASE NR1	$[10^{-39}, 10^{-36}] \text{ GeV}^{-1}$	$[10^{-25}, 10^{-24}]$	$[10^{-14}, 10^{-12}]$
CASE NR2	$[10^{-34}, 10^{-32}] \text{ GeV}^{-1}$	10^{-20}	
Exp. upper bounds	$10^{-10} \text{ GeV}^{-1}$	10^{-13}	10^{-5}

The decay width of the Majoron to two electrons reads [106]

$$\Gamma_{\omega ee} \simeq \frac{1}{8\pi} |\lambda_{\omega ee}|^2 m_\omega, \quad (4.8)$$

where

$$\lambda_{\omega ee} \simeq \frac{1}{8\pi^2} \frac{m_e}{v} \left(\left[\frac{m_D m_D^\dagger}{vv_\chi} \right]_{11} - \frac{1}{2} \text{Tr} \left[\frac{m_D m_D^\dagger}{vv_\chi} \right] \right), \quad (4.9)$$

with $[\dots]_{11}$ standing for the (1, 1) entry of the matrix in the brackets. Substituting explicitly the expression for m_D , the coupling becomes

$$\lambda_{\omega ee} = \frac{1}{16\pi^2} \frac{m_e}{v_\chi} \epsilon_\chi^{\frac{2+2L_N}{L_\chi}} \left([\mathcal{Y}_v \mathcal{Y}_v^\dagger]_{11} - \text{Tr} [\mathcal{Y}_v \mathcal{Y}_v^\dagger] \right). \quad (4.10)$$

Assuming as before that the elements of the product $\mathcal{Y}_v \mathcal{Y}_v^\dagger$ are $\mathcal{O}(1)$ numbers, also the Majoron-electron coupling is predicted to be much smaller than the corresponding experimental bound, as shown in Table 3.

Coupling to neutrinos: Majoron emission in $0\nu\beta\beta$ decays

The tree level couplings of the Majoron to neutrinos does not have an impact only on cosmology, but may be relevant for low-energy terrestrial experiments. In particular, searches for neutrinoless-double-beta decay could also be sensitive to processes in which Majorons are produced, such as in KamLAND-Zen [107] and NEMO-3 [108] experiments.

Current measurements set a lower bound on the half-life of the neutrinoless-double-beta decay of the order of 10^{24} years. In the particular case discussed here, where the Majoron could only be produced by the annihilation of two neutrinos (see Fig. 2), this bound can be translated into a constraint on the Majoron-neutrino coupling [109], such that

$$\lambda_{\omega\nu\nu} < 10^{-5}, \quad (4.11)$$

where $\lambda_{\omega\nu\nu}$ is defined in Eq. (2.13).

The predicted value of the Majoron-neutrino coupling can be read out in Table 3 and it is much smaller than the corresponding experimental value and the bound from Planck [14] ($\lambda_{\omega\nu\nu} < \mathcal{O}(10^{-12})$).

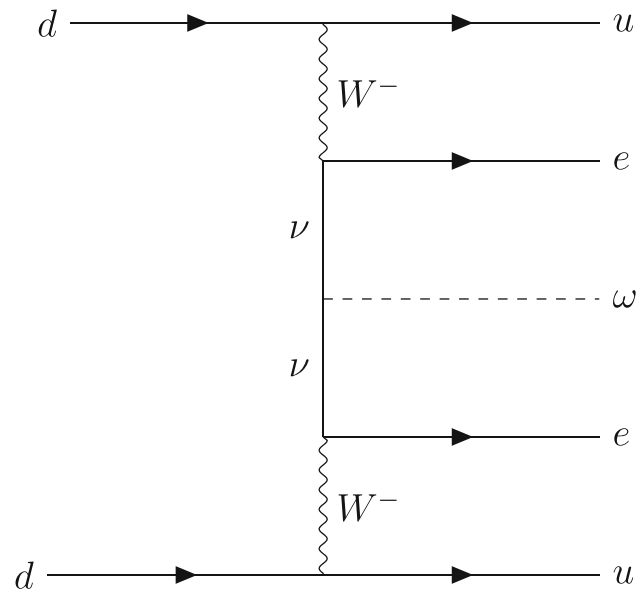


Fig. 2 Feynman Diagram for the neutrinoless-double-beta decay with the emission of a Majoron

Coupling with the SM Higgs: Higgs invisible decay

The Majoron-Higgs coupling follows due to the mixing between the radial component of χ and the physical Higgs, as described at the end of Sect. 2. Indeed, expanding the kinetic term of the field χ , a $\sigma\omega\omega$ coupling arises that induces an effective coupling $h\omega\omega$, via the mixing ϑ . This coupling opens up a new decay channel for the Higgs that contributes to the Higgs invisible decay observable. The width of this process is given by

$$\Gamma_{h \rightarrow \omega\omega} = \frac{s_\vartheta^2 M_h^3}{32\pi v_\chi^2} \lesssim 0.8 \text{ MeV}, \quad (4.12)$$

where the last inequality has been obtained considering that the invisible Higgs decay width may constitute at most the 19% of its total width [110].

This result can be translated into a strong bound on v_χ , that reads

$$\frac{v_\chi}{|s_\vartheta|} \gtrsim 5 \text{ TeV}. \quad (4.13)$$

Table 4 Expectation for the heavy neutrino mass and mixing between heavy and active neutrinos

	$\langle M_N \rangle$	$\sin^2 \theta_s$	$\Gamma_{N \rightarrow 3\nu}^Z$	$\Gamma_{N \rightarrow 3\nu}^\omega$
CASE NR1	[3.5, 200] MeV	$[2.5 \times 10^{-10}, 1.4 \times 10^{-8}]$	$\mathcal{O}(10^{-38})$	$\mathcal{O}(10^{-68})$
CASE NR2	[35.4, 707] GeV	$[7.1 \times 10^{-14}, 1.4 \times 10^{-12}]$	$\mathcal{O}(10^{-27})$	$\mathcal{O}(10^{-66})$

For a light σ , the mixing would be close to its current upper bound, Eq. (2.28), and v_χ should be larger than ~ 1.5 TeV, which would exclude CASE NR2 and part of the parameter space of CASE NR1, see the dashed line in Fig. 1. However, as stated at the end of Sect. 2, the assumption made here is that σ is sufficiently heavy to be integrated out and this corresponds to much smaller values of the mixing angle ϑ , relaxing in this way the bound on v_χ .

4.1 Heavy neutrinos

In both cases discussed in Sect. 2, the heavy neutrino masses lie in ranges that may lead to detection in various experimental facilities. Neutrinos with masses ranging from tens to hundreds of MeV can be probed for and be potentially detected at beam dump or even near detectors of neutrino oscillation experiments [111–118], such as DUNE or SHiP, whereas those with masses in the range of tens to hundreds of GeV have interesting prospects of being produced at the LHC or future colliders [112, 119–125].

On the other hand, given their extremely small couplings, the heavy neutrinos produced in the early Universe would not be Boltzmann suppressed when decoupled from the thermal bath, leading to an unacceptably large contribution to the relativistic degrees of freedom of the Universe after their subsequent decay [126–130]. If their decay takes place before the onset of BBN, the decay products would quickly thermalise and BBN would then proceed as in the standard Λ CDM scenario. However, if the decay of the heavy neutrinos happens after BBN and neutrino decoupling, their contribution to the effective number of neutrinos would be too high and ruled out. If the decay takes place during BBN, the decay products could also alter the production of primordial helium and strong constraints also apply [131–134]. This would be the situation of CASE NR1, for which the neutrino masses and mixings predict decay rates comparable to or larger than the onset of BBN. Conversely, the larger masses that characterize CASE NR2 lead to decays faster than BBN, eluding these cosmological constraints. Hence, BBN and CMB observations disfavor CASE NR1 unless the heavy neutrino decay is faster than BBN in some part of the parameter space or some other modification of the standard Λ CDM scenario is considered. Indeed, if the heavy neutrinos decay after BBN, for heavy neutrino masses in the range [3.5, 200] MeV, then

the bound on the mixing is [130]:

$$\sin^2 \theta_s \equiv \frac{\langle m_\nu \rangle}{\langle M_N \rangle} \lesssim 10^{-15} - 10^{-17}, \quad (4.14)$$

much smaller than the expected value that can be read in Table 4.

5 Conclusions

The Hubble tension may well be due to systematic uncertainties but it might point to a deviation from the Λ CDM model or an extension of the Standard Model of particle physics. In particular, the presence of a Majoron with couplings to the active neutrinos represents an interesting avenue to alleviate this tension. This paper is focussed on a mechanism where neutrino masses and the presence of a Majoron are explained by the spontaneous breaking of Lepton Number. Besides the introduction of three RH neutrinos and a new complex scalar singlet, three sets of Lepton Number charge assignments are identified that correctly explain the lightness of the active neutrinos and provide the Majoron with couplings that lower the Hubble tension from 4.4σ down to 2.5σ .

This mechanism is completely general and could be embedded in different types of flavour models. A compelling case presented here is the embedding in the Minimal (Lepton) Flavour Violating setup: Lepton Number is part of the complete flavour symmetry and therefore naturally arises in this context. The non-Abelian factors are mainly responsible of the intergenerational mass hierarchies and of the mixings, while Lepton Number, besides being associated to the Majoron, is involved in the explanation of the smallness of the active neutrino masses with respect to the top mass. The ratios between the bottom and τ masses can be explained via the spontaneous breaking of the PQ symmetry, which completes the non-Abelian flavour symmetry together with Lepton Number. A QCD axion arises as a byproduct of the PQ symmetry breaking, allowing to solve the Strong CP problem within the same framework.

The Majoron only couples at tree level to neutrinos. The neutrinoless-double-beta decay represents a natural observable where to look for it, but the model prediction turns out to be much smaller than the current experimental sensitivity and much stronger constraints can be derived from its impact in neutrino free streaming and the effective number of neutrino species from CMB observations. Effective couplings to

charged fermions and photons arise at one and two loops, respectively. For this reason, the model is not significantly constrained from CAST and Red Giant observations that otherwise provide stringent bounds for light pseudoscalars.

Due to the mixing between the physical Higgs and the radial degree of freedom of the scalar field producing the Majoron, the latter does couple to the Higgs. This has an impact on the invisible Higgs decay, that indeed provides a strong bound on the VEV of the new scalar, that is, on the Lepton Number breaking scale. However, a natural choice in the model is to assume the radial component to be sufficiently heavy to be integrated out, and correspondingly its mixing with the Higgs gets suppressed, relaxing the bound on the VEV.

Finally, heavy neutrinos are expected to be much lighter than in the traditional type-I Seesaw scenario, in the MeV or GeV ranges depending on the specific case considered. In these mass ranges the decay products of the neutrinos could significantly affect the evolution of the early Universe. Indeed, for masses in the MeV range, decays during Big Bang Nucleosynthesis could alter the production of primordial helium while later decays would imply too large an injection of relativistic species. Conversely, for neutrino masses above the GeV, their decays are typically faster than Big Bang Nucleosynthesis and the decay products thermalise without altering the rest of the thermal history of the Universe. This option is thus preferred with respect to the lighter masses.

The result is a model where fermion masses and mixings can be correctly described, protecting the flavour sector from large deviations from the standard predictions with a new physics scale of the order of a few TeV, solving the strong CP problem and softening at the same time the Hubble tension. This model could be tested indirectly at colliders looking at the invisible Higgs decay and searching for relatively light heavy neutrinos or for the radial component of the scalar field that generates the Majoron.

Acknowledgements The authors acknowledge partial financial support by the Spanish MINECO through the Centro de excelencia Severo Ochoa Program under grant SEV-2016-0597, by the Spanish “Agencia Estatal de Investigación” (AEI) and the EU “Fondo Europeo de Desarrollo Regional” (FEDER) through the projects FPA2016-78645-P and PID2019-108892RB-I00/AEI/10.13039/501100011033. This project has received support from the European Union’s Horizon 2020 research and innovation programme under the Marie Skłodowska-Curie grant agreement No 860881-HIDDeN. L.M. acknowledges partial financial support by the Spanish MINECO through the “Ramón y Cajal” programme (RYC-2015-17173).

Data Availability Statement This manuscript has no associated data or the data will not be deposited. [Authors’ comment: This is a theoretical work, so no datasets have been generated.]

Open Access This article is licensed under a Creative Commons Attribution 4.0 International License, which permits use, sharing, adaptation, distribution and reproduction in any medium or format, as long as you give appropriate credit to the original author(s) and the source, provide

a link to the Creative Commons licence, and indicate if changes were made. The images or other third party material in this article are included in the article’s Creative Commons licence, unless indicated otherwise in a credit line to the material. If material is not included in the article’s Creative Commons licence and your intended use is not permitted by statutory regulation or exceeds the permitted use, you will need to obtain permission directly from the copyright holder. To view a copy of this licence, visit <http://creativecommons.org/licenses/by/4.0/>.

Funded by SCOAP³.

References

1. L. Verde, T. Treu, A. Riess, Tensions Between the Early and the Late Universe (2019). [arXiv:1907.10625](https://arxiv.org/abs/1907.10625)
2. K.C. Wong et al., H0LiCOW XIII. A 2.4% measurement of H_0 from lensed quasars: 5.3 σ tension between early and late-Universe probes (2019). [arXiv:1907.04869](https://arxiv.org/abs/1907.04869)
3. Planck Collaboration, N. Aghanim et al., Planck 2018 Results. VI. Cosmological Parameters (2018). [arXiv:1807.06209](https://arxiv.org/abs/1807.06209)
4. A.G. Riess, S. Casertano, W. Yuan, L.M. Macri, D. Scolnic, Large magellanic cloud cepheid standards provide a 1% foundation for the determination of the hubble constant and stronger evidence for physics beyond Λ CDM. *Astrophys. J.* **876**(1), 85 (2019). [arXiv:1903.07603](https://arxiv.org/abs/1903.07603)
5. M. Archidiacono, S. Gariazzo, C. Giunti, S. Hannestad, R. Hansen, M. Laveder, T. Tram, Pseudoscalar–Sterile neutrino interactions: reconciling the cosmos with neutrino oscillations. *JCAP* **08**, 067 (2016). [arXiv:1606.07673](https://arxiv.org/abs/1606.07673)
6. P. Ko, Y. Tang, Light dark photon and fermionic dark radiation for the hubble constant and the structure formation. *Phys. Lett. B* **762**, 462–466 (2016). [arXiv:1608.01083](https://arxiv.org/abs/1608.01083)
7. E. Di Valentino, C. Bøehm, E. Hivon, F.R. Bouchet, Reducing the H_0 and σ_8 tensions with Dark matter–neutrino interactions. *Phys. Rev. D* **97**(4), 043513 (2018). [arXiv:1710.02559](https://arxiv.org/abs/1710.02559)
8. F. D’Eramo, R.Z. Ferreira, A. Notari, J.L. Bernal, Hot axions and the H_0 tension. *JCAP* **1811**(11), 014 (2018). [arXiv:1808.07430](https://arxiv.org/abs/1808.07430)
9. P. Agrawal, F.-Y. Cyr-Racine, D. Pinner, L. Randall, Rock ‘N’ roll solutions to the hubble tension (2019). [arXiv:1904.01016](https://arxiv.org/abs/1904.01016)
10. P. Agrawal, G. Obied, C. Vafa, H_0 Tension, Swampland conjectures and the Epoch of fading dark matter (2019). [arXiv:1906.08261](https://arxiv.org/abs/1906.08261)
11. S. Alexander, E. McDonough, Axion-dilaton destabilization and the hubble tension. *Phys. Lett. B* **797**, 134830 (2019). [arXiv:1904.08912](https://arxiv.org/abs/1904.08912)
12. S. Ghosh, R. Khatri, T.S. Roy, Dark neutrino interactions phase out the hubble tension (2019). [arXiv:1908.09843](https://arxiv.org/abs/1908.09843)
13. M. Escudero, D. Hooper, G. Krnjaic, M. Pierre, Cosmology with a very light $L_\mu - L_\tau$ Gauge Boson. *JHEP* **03**, 071 (2019). [arXiv:1901.02010](https://arxiv.org/abs/1901.02010)
14. M. Escudero, S.J. Witte, A CMB search for the neutrino mass mechanism and its relation to the hubble tension. *Eur. Phys. J. C* **80**(4), 294 (2020). [arXiv:1909.04044](https://arxiv.org/abs/1909.04044)
15. G.B. Gelmini, A. Kusenko, V. Takhistov, Hints of sterile neutrinos in recent measurements of the hubble parameter (2019). [arXiv:1906.10136](https://arxiv.org/abs/1906.10136)
16. M. Park, C.D. Kreisch, J. Dunkley, B. Hadzhiyska, F.-Y. Cyr-Racine, Λ CDM or self-interacting neutrinos: how CMB data can tell the two models apart. *Phys. Rev. D* **100**(6), 063524 (2019). [arXiv:1904.02625](https://arxiv.org/abs/1904.02625)
17. C.D. Kreisch, F.-Y. Cyr-Racine, O. Doré, The neutrino puzzle: anomalies, interactions, and cosmological tensions. *Phys. Rev. D* **101**(12), 123505 (2020). [arXiv:1902.00534](https://arxiv.org/abs/1902.00534)

18. T.L. Smith, V. Poulin, M.A. Amin, Oscillating scalar fields and the hubble tension: a resolution with novel signatures. *Phys. Rev. D* **101**(6), 063523 (2020). [arXiv:1908.06995](#)
19. Y. Chikashige, R.N. Mohapatra, R. Peccei, Spontaneously broken lepton number and cosmological constraints on the neutrino mass spectrum. *Phys. Rev. Lett.* **45**, 1926 (1980)
20. G. Gelmini, M. Roncadelli, Left-handed neutrino mass scale and spontaneously broken Lepton number. *Phys. Lett. B* **99**, 411–415 (1981)
21. H.M. Georgi, S.L. Glashow, S. Nussinov, Unconventional model of neutrino masses. *Nucl. Phys. B* **193**, 297–316 (1981)
22. J. Schechter, J. Valle, Neutrino decay and spontaneous violation of lepton number. *Phys. Rev. D* **25**, 774 (1982)
23. Z. Chacko, L.J. Hall, T. Okui, S.J. Oliver, CMB signals of neutrino mass generation. *Phys. Rev. D* **70**, 085008 (2004). [arXiv:hep-ph/0312267](#)
24. CMB-S4 Collaboration, K. N. Abazajian et al., *CMB-S4 Science Book*, 1st edn. (2016) [arXiv:1610.02743](#)
25. S. Bashinsky, U. Seljak, Neutrino perturbations in CMB anisotropy and matter clustering. *Phys. Rev. D* **69**, 083002 (2004). [arXiv:astro-ph/0310198](#)
26. E. Masso, F. Rota, G. Zsembinski, On axion thermalization in the early universe. *Phys. Rev. D* **66**, 023004 (2002). [arXiv:hep-ph/0203221](#)
27. A. Salvio, A. Strumia, W. Xue, Thermal axion production. *JCAP* **1401**, 011 (2014). [arXiv:1310.6982](#)
28. R.Z. Ferreira, A. Notari, Observable Windows for the QCD axion through the number of relativistic species. *Phys. Rev. Lett.* **120**(19), 191301 (2018). [arXiv:1801.06090](#)
29. F. Arias-Aragon, F. D'Eramo, R.Z. Ferreira, L. Merlo, A. Notari, Cosmic imprints of xenon1t axions (2020). [arXiv:2007.06579](#)
30. I. Esteban, M. Gonzalez-Garcia, M. Maltoni, T. Schwetz, A. Zhou, The fate of hints: updated global analysis of three-flavor neutrino oscillations (2020). [arXiv:2007.14792](#)
31. C.D. Froggatt, H.B. Nielsen, Hierarchy of quark masses, Cabibbo angles and CP violation. *Nucl. Phys. B* **147**, 277–298 (1979)
32. R. Alonso, A. Urbano, Wormholes and masses for goldstone bosons. *JHEP* **02**, 136 (2019). [arXiv:1706.07415](#)
33. E.K. Akhmedov, Z. Berezhiani, R. Mohapatra, G. Senjanovic, Planck scale effects on the majoron. *Phys. Lett. B* **299**, 90–93 (1993). [arXiv:hep-ph/9209285](#)
34. B.A. Dobrescu, The strong CP problem versus planck scale physics. *Phys. Rev. D* **55**, 5826–5833 (1997). [arXiv:hep-ph/9609221](#)
35. B. Lillard, T.M. Tait, A high quality composite axion. *JHEP* **11**, 199 (2018). [arXiv:1811.03089](#)
36. A. Hook, S. Kumar, Z. Liu, R. Sundrum, The high quality QCD axion and the Lhc. *Phys. Rev. Lett.* **124**(22), 221801 (2020). [arXiv:1911.12364](#)
37. K.R. Dienes, E. Dudas, T. Gherghetta, Invisible axions and large radius compactifications. *Phys. Rev. D* **62**, 105023 (2000). [arXiv:hep-ph/9912455](#)
38. K.-W. Choi, A QCD axion from higher dimensional gauge field. *Phys. Rev. Lett.* **92**, 101602 (2004). [arXiv:hep-ph/0308024](#)
39. P. Cox, T. Gherghetta, M.D. Nguyen, A holographic perspective on the axion quality problem. *JHEP* **01**, 188 (2020). [arXiv:1911.09385](#)
40. H. Fukuda, M. Ibe, M. Suzuki, T.T. Yanagida, A “gauged” $U(1)$ Peccei-Quinn symmetry. *Phys. Lett. B* **771**, 327–331 (2017). [arXiv:1703.01112](#)
41. C.D. Carone, M. Merchand, T' models with high quality fluxions. *Phys. Rev. D* **101**(11), 115032 (2020). [arXiv:2004.02040](#)
42. ATLAS Collaboration, G. Aad et al., Combined measurements of Higgs boson production and decay using up to 80 fb⁻¹ of proton-proton collision data at $\sqrt{s} = 13$ TeV collected with the ATLAS experiment. *Phys. Rev. D* **101**(1), 012002, (2020). [arXiv:1909.02845](#)
43. P.F. Harrison, D.H. Perkins, W.G. Scott, Tri-bimaximal mixing and the neutrino oscillation data. *Phys. Lett. B* **530**, 167 (2002). [arXiv:hep-ph/0202074](#)
44. Z.-Z. Xing, Nearly tri bimaximal neutrino mixing and CP violation. *Phys. Lett. B* **533**, 85–93 (2002). [arXiv:hep-ph/0204049](#)
45. E. Ma, G. Rajasekaran, Softly broken A_4 symmetry for nearly degenerate neutrino masses. *Phys. Rev. D* **64**, 113012 (2001). [arXiv:hep-ph/0106291](#)
46. K.S. Babu, E. Ma, J.W.F. Valle, Underlying A_4 symmetry for the neutrino mass matrix and the quark mixing matrix. *Phys. Lett. B* **552**, 207–213 (2003). [arXiv:hep-ph/0206292](#)
47. G. Altarelli, F. Feruglio, Tri-bimaximal neutrino mixing from discrete symmetry in extra dimensions. *Nucl. Phys. B* **720**, 64–88 (2005). [arXiv:hep-ph/0504165](#)
48. H. Ishimori, T. Kobayashi, H. Ohki, Y. Shimizu, H. Okada, M. Tanimoto, Non-abelian discrete symmetries in particle physics. *Prog. Theor. Phys. Suppl.* **183**, 1–163 (2010). [arXiv:1003.3552](#)
49. G. Altarelli, F. Feruglio, L. Merlo, Tri-bimaximal neutrino mixing and discrete flavour symmetries. *Fortsch. Phys.* **61**, 507–534 (2013). [arXiv:1205.5133](#)
50. D. Hernandez, A. Smirnov, Lepton mixing and discrete symmetries. *Phys. Rev. D* **86**, 053014 (2012). [arXiv:1204.0445](#)
51. W. Grimus, P.O. Ludl, Finite flavour groups of fermions. *J. Phys. A* **45**, 233001 (2012). [arXiv:1110.6376](#)
52. S.F. King, C. Luhn, Neutrino mass and mixing with discrete symmetry. *Rept. Prog. Phys.* **76**, 056201 (2013). [arXiv:1301.1340](#)
53. T2K Collaboration, K. Abe et al., Indication of electron neutrino appearance from an accelerator-produced off-axis muon neutrino beam. *Phys. Rev. Lett.* **107**, 041801 (2011). [arXiv:1106.2822](#)
54. MINOS Collaboration, P. Adamson et al., Improved search for muon-neutrino to electron-neutrino oscillations in minos. *Phys. Rev. Lett.* **107**, 181802 (2011). [arXiv:1108.0015](#)
55. Double Chooz Collaboration, Y. Abe et al., Indication for the disappearance of reactor electron antineutrinos in the double Chooz experiment. *Phys. Rev. Lett.* **108**, 131801 (2012). [arXiv:1112.6353](#)
56. Daya Bay Collaboration, F.P. An et al., Observation of electron-antineutrino disappearance at Daya Bay. *Phys. Rev. Lett.* **108**, 171803 (2012). [arXiv:1203.1669](#)
57. R.E.N.O. Collaboration, J.K. Ahn et al., Observation of reactor electron antineutrino disappearance in the reno experiment. *Phys. Rev. Lett.* **108**, 191802 (2012). [arXiv:1204.0626](#)
58. W. Buchmuller, V. Domcke, K. Schmitz, Predicting θ_{13} and the neutrino mass scale from quark lepton mass hierarchies. *JHEP* **03**, 008 (2012). [arXiv:1111.3872](#)
59. G. Altarelli, F. Feruglio, I. Masina, L. Merlo, Repressing anarchy in neutrino mass textures. *JHEP* **11**, 139 (2012). [arXiv:1207.0587](#)
60. J. Bergstrom, D. Meloni, L. Merlo, Bayesian comparison of $U(1)$ lepton flavor models. *Phys. Rev. D* **89**(9), 093021 (2014). [arXiv:1403.4528](#)
61. G. D'Ambrosio, G.F. Giudice, G. Isidori, A. Strumia, Minimal flavor violation: an effective field theory approach. *Nucl. Phys. B* **645**, 155–187 (2002). [arXiv:hep-ph/0207036](#)
62. V. Cirigliano, B. Grinstein, G. Isidori, M.B. Wise, Minimal flavor violation in the lepton sector. *Nucl. Phys. B* **728**, 121–134 (2005). [arXiv:hep-ph/0507001](#)
63. S. Davidson, F. Palorini, Various definitions of minimal flavour violation for leptons. *Phys. Lett. B* **642**, 72–80 (2006). [arXiv:hep-ph/0607329](#)
64. R. Alonso, G. Isidori, L. Merlo, L.A. Munoz, E. Nardi, Minimal flavour violation extensions of the seesaw. *JHEP* **06**, 037 (2011). [arXiv:1103.5461](#)

65. R. Barbieri, G. Isidori, J. Jones-Perez, P. Lodone, D.M. Straub, $U(2)$ and minimal flavour violation in supersymmetry. *Eur. Phys. J. C* **71**, 1725 (2011). [arXiv:1105.2296](#)
66. G. Blankenburg, G. Isidori, J. Jones-Perez, Neutrino masses and LFV from minimal breaking of $U(3)^5$ and $U(2)^5$ flavor symmetries. *Eur. Phys. J. C* **72**, 2126 (2012). [arXiv:1204.0688](#)
67. F. Arias-Aragón, C. Bouthelier-Madre, J. Cano, L. Merlo, Data driven flavour model (2020). [arXiv:2003.05941](#)
68. R.S. Chivukula, H. Georgi, Composite technicolor standard model. *Phys. Lett. B* **188**, 99–104 (1987)
69. R.D. Peccei, H.R. Quinn, CP conservation in the presence of instantons. *Phys. Rev. Lett.* **38**, 1440–1443 (1977)
70. F. Arias-Aragon, L. Merlo, The minimal flavour violating axion. *JHEP* **10**, 168 (2017). [arXiv:1709.07039](#)
71. R. Alonso, M.B. Gavela, L. Merlo, S. Rigolin, On the scalar potential of minimal flavour violation. *JHEP* **07**, 012 (2011). [arXiv:1103.2915](#)
72. R. Alonso, M.B. Gavela, D. Hernandez, L. Merlo, On the potential of leptonic minimal flavour violation. *Phys. Lett. B* **715**, 194–198 (2012). [arXiv:1206.3167](#)
73. R. Alonso, M.B. Gavela, D. Hernández, L. Merlo, S. Rigolin, Leptonic dynamical Yukawa couplings. *JHEP* **08**, 069 (2013). [arXiv:1306.5922](#)
74. R. Alonso, M.B. Gavela, G. Isidori, L. Maiani, Neutrino mixing and masses from a minimum principle. *JHEP* **11**, 187 (2013). [arXiv:1306.5927](#)
75. B. Grinstein, V. Cirigliano, G. Isidori, M.B. Wise, Grand unification and the principle of minimal flavor violation. *Nucl. Phys. B* **763**, 35–48 (2007). [arXiv:hep-ph/0608123](#)
76. B. Grinstein, M. Redi, G. Villadoro, Low scale flavor gauge symmetries. *JHEP* **11**, 067 (2010). [arXiv:1009.2049](#)
77. T. Feldmann, See-Saw masses for quarks and leptons in $SU(5)$. *JHEP* **04**, 043 (2011). [arXiv:1010.2116](#)
78. D. Guadagnoli, R.N. Mohapatra, I. Sung, Gauged flavor group with left-right symmetry. *JHEP* **04**, 093 (2011). [arXiv:1103.4170](#)
79. M. Redi, A. Weiler, Flavor and CP invariant composite Higgs models. *JHEP* **11**, 108 (2011). [arXiv:1106.6357](#)
80. A.J. Buras, L. Merlo, E. Stamou, The impact of flavour changing neutral gauge Bosons on $\bar{B} \rightarrow X_s \gamma$. *JHEP* **08**, 124 (2011). [arXiv:1105.5146](#)
81. A.J. Buras, M.V. Carlucci, L. Merlo, E. Stamou, Phenomenology of a gauged $SU(3)^3$ flavour model. *JHEP* **03**, 088 (2012). [arXiv:1112.4477](#)
82. R. Alonso, M.B. Gavela, L. Merlo, S. Rigolin, J. Yepes, Minimal flavour violation with strong Higgs dynamics. *JHEP* **06**, 076 (2012). [arXiv:1201.1511](#)
83. R. Alonso, M.B. Gavela, L. Merlo, S. Rigolin, J. Yepes, Flavor with a light dynamical “Higgs Particle”. *Phys. Rev. D* **87**(5), 055019 (2013). [arXiv:1212.3307](#)
84. L. Lopez-Honorez, L. Merlo, Dark matter within the minimal flavour violation Ansatz. *Phys. Lett. B* **722**, 135–143 (2013). [arXiv:1303.1087](#)
85. L. Merlo, S. Rosauero-Alcaraz, Predictive leptogenesis from minimal lepton flavour violation. *JHEP* **07**, 036 (2018). [arXiv:1801.03937](#)
86. G. Isidori, Y. Nir, G. Perez, Flavor physics constraints for physics beyond the standard model. *Ann. Rev. Nucl. Part. Sci.* **60**, 355 (2010). [arXiv:1002.0900](#)
87. S. King, Large mixing angle MSW and atmospheric neutrinos from single right-handed neutrino dominance and $U(1)$ family symmetry. *Nucl. Phys. B* **576**, 85–105 (2000). [arXiv:hep-ph/9912492](#)
88. E. Bertuzzo, P. Di Bari, F. Feruglio, E. Nardi, Flavor symmetries, leptogenesis and the absolute neutrino mass scale. *JHEP* **11**, 036 (2009). [arXiv:0908.0161](#)
89. D. Aristizabal Sierra, F. Bazzocchi, I. de Medeiros Varzielas, L. Merlo, S. Morisi, Tri-bimaximal lepton mixing and leptogenesis. *Nucl. Phys. B* **827**, 34–58 (2010). [arXiv:0908.0907](#)
90. V. Cirigliano, B. Grinstein, Phenomenology of minimal lepton flavor violation. *Nucl. Phys. B* **752**, 18–39 (2006). [arXiv:hep-ph/0601111](#)
91. M.B. Gavela, T. Hambye, D. Hernandez, P. Hernandez, Minimal flavour seesaw models. *JHEP* **09**, 038 (2009). [arXiv:0906.1461](#)
92. R. Alonso, E. Fernandez Martínez, M. B. Gavela, B. Grinstein, L. Merlo, P. Quilez, Gauged lepton flavour. *JHEP* **12**, 119 (2016). [arXiv:1609.05902](#)
93. D.N. Dinh, L. Merlo, S.T. Petcov, R. Vega-Álvarez, Revisiting minimal lepton flavour violation in the light of leptonic CP violation. *JHEP* **07**, 089 (2017). [arXiv:1705.09284](#)
94. V. Baluni, CP violating effects in QCD. *Phys. Rev. D* **19**, 2227–2230 (1979)
95. R. Crewther, P. Di Vecchia, G. Veneziano, E. Witten, Chiral estimate of the electric dipole moment of the neutron in quantum chromodynamics. *Phys. Lett. B* **88**, 123 (1979). [Erratum: *Phys.Lett.B* **91**, 487 (1980)]
96. nEDM Collaboration, C. Abel et. al., Measurement of the permanent electric dipole moment of the neutron. *Phys. Rev. Lett.* **124**(8), 081803 (2020). [arXiv:2001.11966](#)
97. F. Wilczek, Problem of strong P and T invariance in the presence of instantons. *Phys. Rev. Lett.* **40**, 279–282 (1978)
98. S. Weinberg, A new light boson? *Phys. Rev. Lett.* **40**, 223–226 (1978)
99. G. Grilli di Cortona, E. Hardy, J. Pardo Vega, G. Villadoro, The QCD axion, precisely. *JHEP* **01**, 034 (2016). [arXiv:1511.02867](#)
100. J. Jaeckel, M. Spannowsky, Probing MeV to 90 GeV axion-like particles with Lep and Lhc. *Phys. Lett. B* **753**, 482–487 (2016). [arXiv:1509.00476](#)
101. M. Bauer, M. Neubert, A. Thamm, Collider probes of axion-like particles. *JHEP* **12**, 044 (2017). [arXiv:1708.00443](#)
102. CAST Collaboration, V. Anastassopoulos et. al., New cast limit on the axion-photon interaction. *Nat. Phys.* **13**, 584–590 (2017). [arXiv:1705.02290](#)
103. N. Viaux, M. Catelan, P.B. Stetson, G. Raffelt, J. Redondo, A.A.R. Valcarce, A. Weiss, Neutrino and axion bounds from the globular cluster M5 (NGC 5904). *Phys. Rev. Lett.* **111**, 231301 (2013). [arXiv:1311.1669](#)
104. O. Straniero, I. Dominguez, M. Giannotti, A. Mirizzi, Axion-electron coupling from the RGB tip of globular clusters. In *13th Patras Workshop on Axions, WIMPs and WISPs* (2018), pp. 172–176. [arXiv:1802.10357](#)
105. S.A. Díaz, K.-P. Schröder, K. Zuber, D. Jack, E.E.B. Barrios, Constraint on the Axion-Electron coupling constant and the neutrino magnetic dipole moment by using the tip-RGB luminosity of fifty globular clusters (2019). [arXiv:1910.10568](#)
106. C. García-Cely, J. Heeck, Neutrino lines from majoron dark matter. *JHEP* **05**, 102 (2017). [arXiv:1701.07209](#)
107. KamLAND-Zen Collaboration, A. Gando et. al., Search for Majorana neutrinos near the inverted mass hierarchy region with Kamland-Zen. *Phys. Rev. Lett.* **117**(8), 082503 (2016). [arXiv:1605.02889](#) [Addendum: *Phys.Rev.Lett.* **117**, 109903 (2016)]
108. R. Arnold et al., Final results on ^{82}Se double beta decay to the ground state of ^{82}Kr from the NEMO-3 experiment. *Eur. Phys. J. C* **78**(10), 821 (2018). [arXiv:1806.05553](#)
109. R. Cepedello, F.F. Deppisch, L. González, C. Hati, M. Hirsch, Neutrinoless double- β decay with nonstandard majoron emission. *Phys. Rev. Lett.* **122**(18), 181801 (2019). [arXiv:1811.00031](#)
110. CMS Collaboration, A.M. Sirunyan et al., Search for invisible decays of a Higgs Boson produced through vector boson fusion in proton–proton collisions at $\sqrt{s} = 13$ TeV. *Phys. Lett. B* **793**, 520–551 (2019). [arXiv:1809.05937](#)

111. D. Gorbunov, M. Shaposhnikov, How to find neutral leptons of the ν MSM? JHEP **10**, 015 (2007). [arXiv:0705.1729](#) [Erratum: JHEP **11**, 101 (2013)]
112. A. Atre, T. Han, S. Pascoli, B. Zhang, The search for heavy majorana neutrinos. JHEP **05**, 030 (2009). [arXiv:0901.3589](#)
113. K. Bondarenko, A. Boyarsky, D. Gorbunov, O. Ruchayskiy, Phenomenology of GeV-scale heavy neutral leptons. JHEP **11**, 032 (2018). [arXiv:1805.08567](#)
114. SHiP Collaboration, C. Ahdida et al., Sensitivity of the SHiP experiment to heavy neutral leptons. JHEP **04**, 077 (2019). [arXiv:1811.00930](#)
115. K. Bondarenko, A. Boyarsky, M. Ovchinnikov, O. Ruchayskiy, Sensitivity of the intensity frontier experiments for neutrino and scalar portals: analytic estimates. JHEP **08**, 061 (2019). [arXiv:1902.06240](#)
116. P. Ballett, T. Boschi, S. Pascoli, heavy neutral leptons from low-scale seesaws at the DUNE near detector. JHEP **20**, 111 (2020). [arXiv:1905.00284](#)
117. J.M. Berryman, A. de Gouvea, P.J. Fox, B.J. Kayser, K.J. Kelly, J.L. Raaf, Searches for decays of new particles in the DUNE multi-purpose near detector. JHEP **02**, 174 (2020). [arXiv:1912.07622](#)
118. P. Coloma, E. Fernández-Martínez, M. González-López, J. Hernández-García, Z. Pavlovic, GeV-scale neutrinos: interactions with mesons and DUNE sensitivity (2020). [arXiv:2007.03701](#)
119. F. del Aguila, J. Aguilar-Saavedra, Distinguishing seesaw models at LHC with multi-lepton signals. Nucl. Phys. B **813**, 22–90 (2009). [arXiv:0808.2468](#)
120. S. Antusch, O. Fischer, Testing sterile neutrino extensions of the Standard Model at future lepton colliders. JHEP **05**, 053 (2015). [arXiv:1502.05915](#)
121. F.F. Deppisch, P. Bhupal Dev, A. Pilaftsis, Neutrinos and collider physics. New J. Phys. **17**(7), 075019 (2015). [arXiv:1502.06541](#)
122. S. Antusch, E. Cazzato, O. Fischer, Sterile neutrino searches at future e^-e^+ , pp , and e^-p colliders. Int. J. Mod. Phys. A **32**(14), 1750078 (2017). [arXiv:1612.02728](#)
123. Y. Cai, T. Han, T. Li, R. Ruiz, Lepton number violation: Seesaw models and their collider tests. Front. Phys. **6**, 40 (2018). [arXiv:1711.02180](#)
124. P. Bhupal Dev, Y. Zhang, Displaced vertex signatures of doubly charged scalars in the type-II seesaw and its left-right extensions. JHEP **10**, 199 (2018). [arXiv:1808.00943](#)
125. S. Pascoli, R. Ruiz, C. Weiland, Heavy neutrinos with dynamic jet vetoes: multilepton searches at $\sqrt{s} = 14, 27$, and 100 TeV. JHEP **06**, 049 (2019). [arXiv:1812.08750](#)
126. K. Sato, M. Kobayashi, Cosmological constraints on the mass and the number of heavy lepton neutrinos. Prog. Theor. Phys. **58**, 1775 (1977)
127. J. Gunn, B. Lee, I. Lerche, D. Schramm, G. Steigman, Some astrophysical consequences of the existence of a heavy stable neutral lepton. Astrophys. J. **223**, 1015–1031 (1978)
128. P. Hernandez, M. Kekic, J. Lopez-Pavon, Low-scale seesaw models versus N_{eff} . Phys. Rev. D **89**(7), 073009 (2014). [arXiv:1311.2614](#)
129. P. Hernandez, M. Kekic, J. Lopez-Pavon, N_{eff} in low-scale seesaw models versus the lightest neutrino mass. Phys. Rev. D **90**(6), 065033 (2014). [arXiv:1406.2961](#)
130. A.C. Vincent, E.F. Martínez, P. Hernández, M. Lattanzi, O. Mena, Revisiting cosmological bounds on sterile neutrinos. JCAP **04**, 006 (2015). [arXiv:1408.1956](#)
131. A. Dolgov, S. Hansen, G. Raffelt, D. Semikoz, Cosmological and astrophysical bounds on a heavy sterile neutrino and the KARMEN anomaly. Nucl. Phys. B **580**, 331–351 (2000). [arXiv:hep-ph/0002223](#)
132. O. Ruchayskiy, A. Ivashko, Restrictions on the lifetime of sterile neutrinos from primordial nucleosynthesis. JCAP **10**, 014 (2012). [arXiv:1202.2841](#)
133. G.B. Gelmini, M. Kawasaki, A. Kusenko, K. Murai, V. Takhistov, Big bang nucleosynthesis constraints on sterile neutrino and lepton asymmetry of the Universe (2020). [arXiv:2005.06721](#)
134. A. Boyarsky, M. Ovchinnikov, O. Ruchayskiy, V. Syvolap, Improved BBN constraints on heavy neutral leptons (2020). [arXiv:2008.00749](#)